Faint Near-Neighbor Detection with a Fiber Nuller

E. Serabyn
Jet Propulsion Laboratory, MS 171-113
California Institute of Technology
4800 Oak Grove Drive
Pasadena, CA 91109

Abstract—Direct detection of nearby extra-solar planets via their thermal infrared emission can be carried out by means of infrared nulling interferometry. In this approach, the central star is nulled, while the emission from off-axis sources is transmitted and modulated by the rotation of the off-axis fringes. Because of the high contrasts involved, and the novelty of the measurement technique, it is essential to gain experience with this technique before launch of potential missions such as the Terrestrial Planet Finder Interferometer (TPF-I). Here a simple ground-based experiment that can test the essential aspects of the TPF signal measurement and image reconstruction approaches is described. It is based on generating a rotating interferometric baseline within the pupil of a large single-aperture telescope. This approach should allow for testing of proposed signal extraction algorithms for the detection of single and multiple near-neighbor companions, and also allows for the development and deployment of potential nulling beam combiners. Interestingly, such an interferometric nuller on a single aperture telescope also functions as a coronagraph with a rather small inner working distance. Such a "nulling coronagraph" can thus outperform classical coronagraphs in certain respects.

1. INTRODUCTION

To enable the direct detection of faint companions very near bright stars, techniques such as single-aperture coronagraphy and multiple-aperture nulling interferometry [1-3] are being developed. However, nulling interferometry differs from normal long-baseline interferometry in one important respect - the need to maintain a fixed-phase null implies that the complex visibility of the source brightness distribution is not directly measurable. What is measured is the flux transmitted by the instantaneous fringe pattern, so that direct Fourier inversion to the source plane is not possible. More indirect inversion techniques are thus likely necessary [2].

As the nulling interferometer rotates, the fringe pattern centered on the star also rotates (Fig. 1). As it does so, the fringes sweep across the position of any off-axis companion, modulating its transmitted flux. At larger off-axis angles, more fringes cross the companion's position, and so higher harmonics arise in the detected signal (Fig. 2). The harmonic content of the signal thus determines the companion's radial offset, and the azimuth of the transmission maximum determines its azimuth.

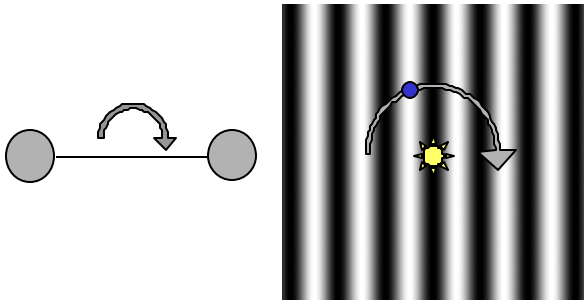

Figure 1. Schematic of a rotating long-baseline nuller and the accompanying fringe pattern. Destructive interference is maintained at the stellar position as the baseline and fringe pattern rotate. Flux from off-axis companions is modulated as the transmission fringes sweep past.

In the simplest case of a single-baseline nuller, the fringe transmission is given by

$$T(\chi) = \sin^2(\chi/2) = (1-\cos(\chi))/2, \qquad (1)$$

where χ is the relative phase between the two telescopes. For a given instantaneous orientation of the baseline vector, $\mathbf{b}$, and a point located at the vector angular position $\mathbf{q}$ in the fixed (θ,φ) coordinate system on the sky, χ is given by

$$\chi = k\mathbf{b}\cdot\mathbf{q} = kb\theta\cos(\varphi-\alpha), \qquad (2)$$

where α is the interferometer rotation angle. This implies that the instantaneous fringe transmission pattern is given by

$$T(\theta,\varphi,\alpha) = (1 - \cos(kb\theta\cos(\varphi-\alpha)))/2. \qquad (3)$$

The transmission vs. rotation angle is plotted for two radial offsets in Fig. 2, where the increased importance of higher harmonics at larger off-axis distances is evident. Equation 3 can be expanded in a series of Bessel functions, J_n, of order

n. For a constant rotation rate, ω, we have $\alpha = \omega t$, and the signal consists of a series of harmonics of the frequency 2ω.

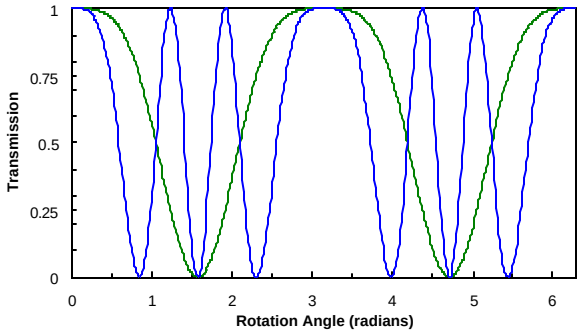

Figure 2. Signal from an off-axis source transmitted by a rotating single-baseline nuller. The thick green line is for a source at $\lambda/2b$, and the thin blue line for a source at $3\lambda/2b$. In both cases, the source is at zero azimuth.

Given the novelty of a rotating long-baseline nuller, and the ambiguity inherent in image reconstruction without full complex visibility data, it would clearly be very valuable to verify both the viability of the basic approach and the robustness of potential signal reconstruction algorithms by means of ground-based demonstrations prior to launch. We are therefore implementing a rotating nuller within the pupil of a single ground-based telescope, by establishing an interferometric baseline between separated sub-apertures within the common telescope pupil (Fig. 3). In the course of these considerations, it became clear that such an approach also provides a novel and capable coronagraph. In the following, we describe potential implementations and potential advantages of such an approach.

2. IMPLEMENTING A ROTATING NULLER

A number of different nulling beam-combination schemes can be used to null two beams, including classical beamsplitter-based systems, injection into a common fiber (the "fiber nuller"), and cross-coupling between fibers (Fig. 4). The classical beamsplitter-based approach (Fig. 4; A) has a number of well known variants with one or two beamsplitters [3], and the fiber cross-coupler (Fig. 4; C) [4]

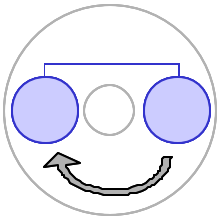

Figure 3. Rotating single baseline nuller (blue) within the pupil of a single-aperture telescope (gray outline). The light from the two sub-apertures is combined interferometrically in a nulling beam-combiner. The light from the area outside the sub-apertures is not collected.

tends to have dispersion issues. The relatively novel fiber nuller (Fig. 4; B) is based on the injection of a number of beams into a common single-mode fiber in the focal plane [5,6]. Deep nulling of monochromatic light to close to the 10^{-6} level has now been demonstrated with a fiber nuller [6]. For more broadband nulling, an achromatic phase shifter to introduce a π radian phase shift between the two beams [7] is needed. Solutions for glass dispersion correctors are straightforward, and Fig. 5 shows a solution for CaF_2 glass that produces deep nulls across the K-band (2.2 μm). However, a fiber nuller beam combiner has not yet been used for on-sky observations.

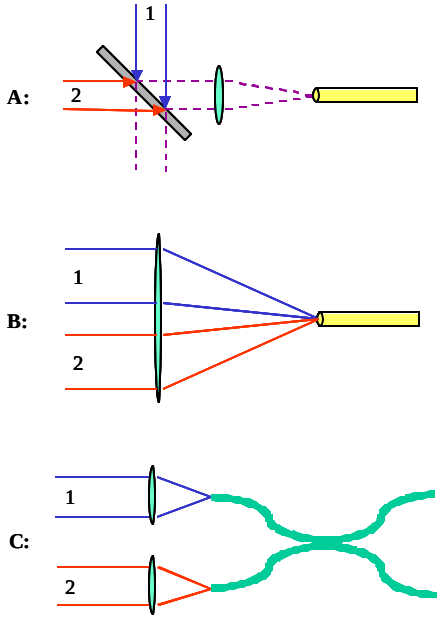

Figure 4. Schematic of the three possible types of nulling beam combiner. A: combination of beams at a beamsplitter. B: combination of beams at a fiber tip (the fiber nuller). C: combination by cross-coupling between fibers. In the fiber nuller, two spatially separated beams are focused onto a common single-mode fiber by a common optic. For all cases, a relative phase shift of $\pi/2$ or π radians is applied by an achromatic phase shifter (not shown). In some cases, an achromatic $\pi/2$ phase shift is also supplied by the beam splitter.

Baseline rotation can in principle be accomplished either with a rotating dual aperture mask, or by passing the beam through a pupil rotator, such as a K-mirror. The first option leads to a number of rotating beams after the sub-aperture mask, and so the nulling beamcombiner must be able to deal with lateral beam motion. Only the fiber nuller seems a natural match to such a contingency, since in this case, both beams are within the broad fiber acceptance cone, and so the baseline between the sub-apertures can have any orientation This leads to a very simple configuration for the rotating-baseline nuller, shown as case I in Fig. 6.

However, in this approach, the achromatic phase shifter would either need to rotate with the sub-aperture mask, or it would be necessary to accept a large dead zone in rotation angle as the sub-apertures transition across the phase step. Neither of these solutions is ideal, but nevertheless, they provide simple and feasible nulling solutions that are also quick to implement. The disadvantage of a rotating phase shifter can be obviated if a pupil rotator, such as a K-mirror, were to be used instead, in which case a fixed dual-aperture mask could define the rotating sub-apertures (Fig. 6, cases IIa and IIb. Case IIa is still a fiber nuller but case IIb is now a beamsplitter-based nuller. In such an approach, the selected rotating sub-aperture beams now lie exclusively upstream of the K-mirror, and the downstream nulling optics thus need only accommodate fixed beams. The upstream beams are of course free to rotate within the larger telescope pupil.

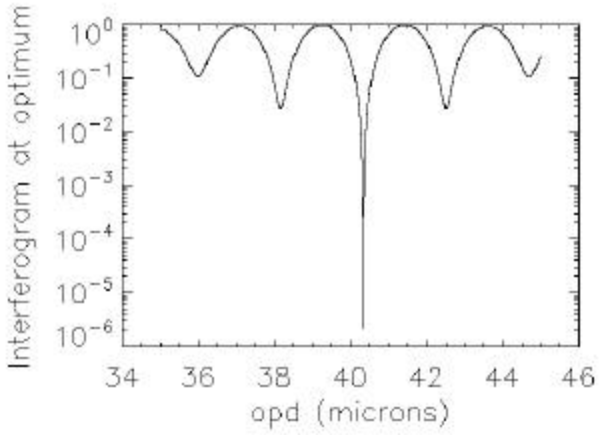

Figure 5. Null depths attainable with a CaF_2 glass phase shifter in the K-band.

While a fiber nuller can be used with a fixed sub-aperture mask as well (Case IIa), so can more classical beamsplitter-based nulling beamcombiners. Indeed, as indicated by cases IIa and IIb of Fig. 8, any type of nuller can follow the pupil rotator and the fixed subaperture mask. This provides a high degree of flexibility, as a number of familiar nulling beam-combiner configurations can then be considered, including fiber nullers, single beamsplitters, and dual-beamsplitter-based configurations such as rotational shearing interferometers, and dual-beam Mach-Zehnder, Sagnac and Michelson interferometers [3]. In the classical beamsplitter-based case, the light from the combined beam can be focused into a fiber with high efficiency, thus avoiding the losses inherent in the fiber nuller approach.

Finally, by reversing the order of the pupil mask and nuller, a single-aperture mask can be used to define both of the pair of sub-apertures, because in reverse propagation, the nulling beamcombiner generates two initial beams out of the one final combined beam. In this configuration, different nulling beamcombiners can also be considered, but one choice which is easy to visualize is a symmetric rotational shearing interferometer (RSI). An RSI, for example, provides several advantages. First, since RSIs combine two pupil images rotated by 180 degrees, all baselines centered on the pupil are generated simultaneously. A number of baselines can then be accessed simultaneously by means of different off-axis subapertures feeding different fibers, thus achieving pupil efficiencies approaching unity. Second, each baseline is duplicated on the opposite side of the center in the recombined pupil. This duplicate baseline can be made use of for e.g., a second waveband, or for phase measurement and control. Other nulling beam-combiner configurations, such as dual-beam Mach-Zehnder or Sagnac interferometers, can also be used, with a similar, but not identical, set of advantages. Clearly, a wide range of nulling beamcombiner configurations can be employed with a rotating nuller.

4. BASIC PERFORMANCE

How well can a rotating sub-aperture nuller on a large ground-based telescope perform? The main questions are the inner working distance (IWD), i.e., the smallest angular offset at which a companion can be detected, the achievable contrast vs. radial offset, and the sensitivity loss due to the collecting area reduction. The IWD is given by IWD = $\alpha\lambda/2b$, where λ is the wavelength, b the baseline length, and α is a constant of order unity. There is a certain freedom in determining α, and different potential choices range from e.g., the fringe half-power point, $\alpha = 0.5$, to just under unity ($\alpha \approx 0.85$) if the central-most region where off-axis companions start to undergo cancellation is to be avoided.

Since the maximum baseline length available within the single aperture telescope pupil is D - s, where D is the aperture diameter and s the sub-aperture diameter, we have IWD = $\alpha\lambda/(2(D-s))$. If we take s=D/3 to avoid the central obscuration, we get IWD = $0.75\alpha\lambda/D$. Thus, independent of the exact value of α, the IWD is significantly smaller ($\approx 0.5\lambda/D$) than that of a classical coronagraph (several λ/D), so that a rotating nuller using only part of the full pupil can in principle be used for observations closer to the optical axis than a classical coronagraph utilizing the full telescope pupil.

On the other hand, the diameter of the field of view, FOV, is set by the width of the subaperture beam coupling to the single mode fiber. A smaller sub-aperture comes with an increased FOV, since FOV $\approx \lambda/s$. In general, FOV/IWD = $2(D-s)/(\alpha s)$. For s = D/3, the case discussed earlier, FOV $\approx 3\lambda/D$, and FOV/IWD = $4/\alpha$. The accessible angles are thus restricted by the finite FOV, but they cover a range otherwise inaccessible, and so very useful, at small radial offsets from the center.

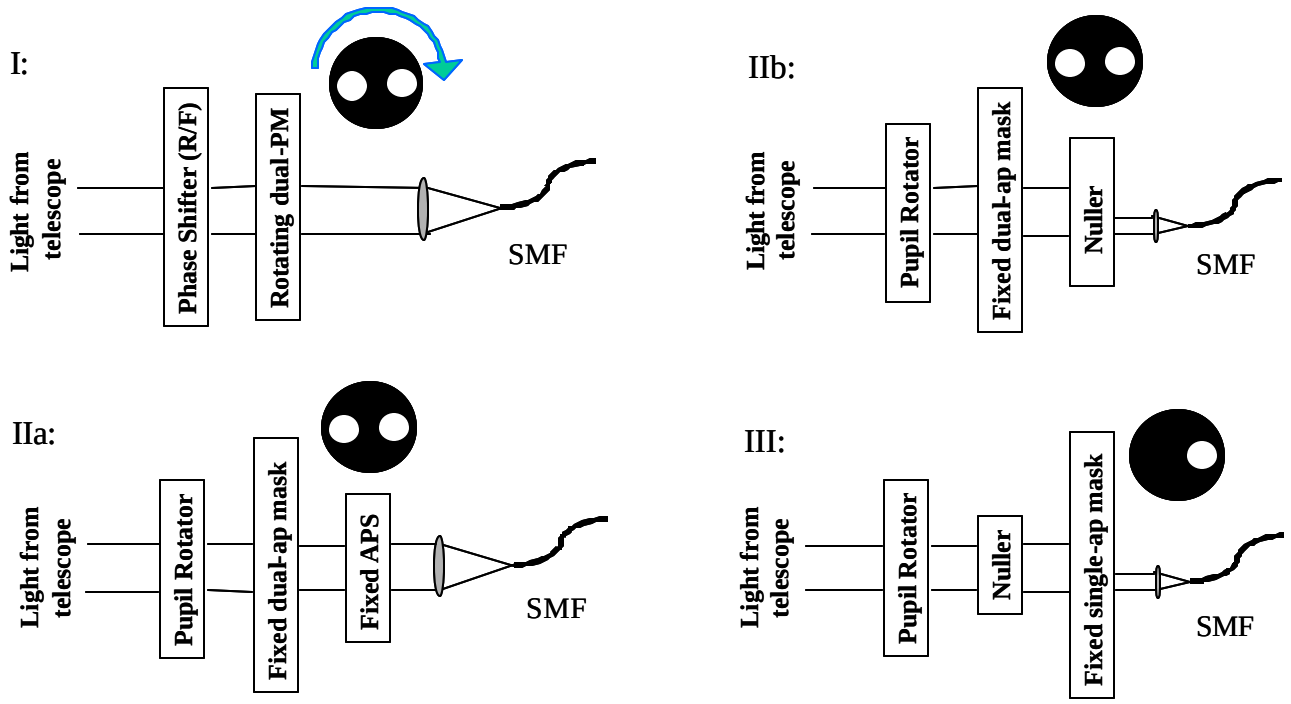

Figure 6. Four potential layouts for a rotating nuller on a single-aperture telescope. R/F means "rotating or fixed", PM is "pupil mask", APS is "achromatic phase shifter", SMF is "single mode filter", and "ap" is short for "aperture". In version III, only a single subaperture is necessary, although more subapertures could be used to increase efficiency or to lay out different pupil-plane configurations.

In particular, given the large photon fluxes available in the near-infrared, the timescale for collecting enough photons for the phase measurement can be quite short. The accuracy of a phase measurement is given by the familiar formula, $\varphi \approx 1/\mathrm{SNR}$, where small factors of order unity have been ignored. In the signal-dominated case, the SNR is the square root of the number of detected stellar photons per measurement cycle, which is given by Rt, where R is the detection rate and t the integration time. Since the null depth is given by the square of half the phase error, the attainable null depth, N, is inversely proportional to the detection rate of incident stellar photons. Allowing for phase measurements at a wavelength half that of the nulling band (e.g., J-band vs. K band), the result is that $t = 1/(16 R_J N)$. Thus even allowing for a J-band transmission of order 0.1, the phase accuracy needed to maintain a null of order 10^{-4} can be obtained on a 5th mag star in a time of order 10^{-4} sec, well below atmospheric coherence timescales.

Indeed, in interferometers with multiple outputs, the phase measurement can become fairly straightforward. For example, because dual copies of any baseline are available in an RSI, one of the dual outputs can be used to measure and stabilize the phase of the second output, which is held fixed at null. Additional SNR improvements are also possible, by means of the inclusion of additional output ports sampling different baseline lengths. In particular, source reconstruction would be eased by the addition of output sub-apertures covering a range of baseline lengths (e.g., Fig. 11).

6. The Role of the Spatial Filter

It is important to emphasize the key role that the final spatial filter plays. For both linear and rotational shearing interferometers, tip-tilt errors degrade the central stellar null with a θ^2 dependence. In contrast, if a single-mode fiber is used to spatially filter the focal plane field, tip-tilt errors do not have as large an impact. In this case, tip-tilt errors affect the coupling of the starlight to the fiber, and so are translated into intensity changes. This converts the null sensitivity to a θ^4 dependence. This was discussed in [8], but can be easily seen to be the case from the basic transmission properties of single-mode fibers, which only allow the propagation of fields oriented perpendicular to the propagation direction. For a field incident at angle θ, the $\sin\theta$ component along the axis of the fiber thus cannot propagate, because that field component is parallel to the fiber axis. Therefore, the linear residual field component, which would lead to a θ^2 intensity leakage term, cannot propagate in the fiber. On the other hand, the perpendicular field component, which goes as $\cos\theta$, can propagate in the fiber, which leads to a field leakage of $1-\cos\theta$. For small θ, the residual power leakage is then proportional to θ^4. Therefore, in the presence

of a given level of tip-tilt errors, a single-mode fiber spatial filter in the focal plane is able to provide a much more stable, and hence deeper, level of starlight rejection. Thus, the application of fibers to telescope-based nullers is one of the goals of our work.

In addition, it is because of the single-mode fiber that one needs only measure the single phase offset between the two sub-aperture beams to achieve improved nulls. Again, the fiber erases the sub-pupil tip-tilt residuals, leaving on-axis propagation. Thus, the only phase-related quantity that survives propagation through the fiber is the average phase offset between the two incident fields. The fiber thus also greatly simplifies control issues, by reducing the number of control parameters to a single relative phase, and so provides for a much more robust measurement approach.

7. SUMMARY

Rotating space-based nulling interferometers will not only involve many new technologies, but also new signal measurement approaches and image reconstruction techniques. As such, it is highly desirable to test these approaches prior to the launch of any multi-aperture interferometric nuller. One way to test potential signal measurement and reconstruction approaches is with a rotating sub-aperture nuller operating within the pupil of a single ground-based telescope, as is described here. However, in addition to simply testing interferometric approaches, it turns out that such a rotating nuller will also provide a very capable coronagraph, with a high dynamic range and a small inner working angle, thus providing a scientific justification for building and using such a device on an existing ground-based telescope. The potential for novel scientific observations at small inner working angles will be essential to obtain the observing time needed to test this approach on ground-based telescopes.

The desired nulling coronagraph can be implemented in a number of ways, from a simple rotating pupil mask with a fiber combiner, to more complex and capable systems which begin with a pupil rotator, and are followed with any type of nuller. The expected performance depends heavily on the level of phase correction, but even with the simplest approach, that of simply relying on an existing AO system, the approach can begin to be validated with observations of binary stars of low contrast. In fact, with improvements expected with next generation AO systems, an order of magnitude performance improvement is possible. On the other hand, inclusion of phase measurement and correction between the sub-apertures can provide the control level needed to obtain stable nulls at the 10^{-3} to 10^{-4} level in the 2 μm K-band. With this level of performance, the signal extraction and image reconstruction approaches being considered for space based nulling interferometers can be tested under real astronomical observing conditions, thus providing a greatly improved level of confidence in the rotating nulling interferometer approach.

This work was carried out at the Jet Propulsion Laboratory, California Institute of Technology, under contract with the National Aeronautics and Space Administration

REFERENCES

[1] R.N. Bracewell 1978, "Detecting nonsolar planets by spinning infrared interferometer," Nature 274, 780.

[2] J.R.P.Angel and N.J. Woolf 1997, "An imaging nulling interferometer to study extrasolar planets," Astrophys. J. 475, 373

[3] E. Serabyn 2003, "Nulling Interferometry Progress," in Proc. SPIE 4838, 594

[4] V. Weber et al. 2004, "Nulling interferometer based on an integrated optics combiner," in Proc. SPIE 5491, 842

[5] O. Wallner, J.M.P. Armengol and A. Karlsson 2004, "Multi-axial single-mode beam combiner," in Proc. SPIE 5491, 798

[6] P. Haguenauer and E. Serabyn, 2006, "Deep nulling of laser light with a single-mode fiber beam combiner," Applied Optics, 45, 2749

[7] R. Angel 1989, "Use of a 16m telescope to detect earthlike planets," in "The Next Generation Space Telescope," STScI, p. 81

[8] B. Mennesson et al. 2002, JOSA 19, 596